Karbala International Journal of Modern Science

Volume 8 | Issue 4 Article 11

An Enhanced Diabetic Foot Ulcer Classification Approach Using GLCM and Deep Convolution Neural Network

Hussein A. Ismael
College of Information Technology, University of Babylon, Hillah, Babil,, husseinyessari@uobabylon.edu.iq

Nabeel H. Al-A'araji
College of Information Technology, University of Babylon, Hillah

Baheja khudair shukur
College of Computer Science & Information Technology, University of Kerbala, Kerbala, Iraq

Recommended Citation
Ismael, Hussein A.; Al-A'araji, Nabeel H.; and shukur, Baheja khudair (2022) "An Enhanced Diabetic Foot Ulcer Classification Approach Using GLCM and Deep Convolution Neural Network," *Karbala International Journal of Modern Science*: Vol. 8 : Iss. 4 , Article 11.
Available at: https://doi.org/10.33640/2405-609X.3268

An Enhanced Diabetic Foot Ulcer Classification Approach Using GLCM and Deep Convolution Neural Network

Abstract

Diabetic Foot Ulcers (DFU) are considered to be a common complication of diabetes, usually resulting in the amputation of lower extremities. Therefore, diagnosing this disease at an early stage is necessary to avoid the accompanying treatment approach, and this results in a significant cost reduction for the patient. To achieve an early diagnosis of this disease, we need to classify a patient's skin as normal or abnormal. A classification process relies heavily on the extracted features. So, we proposed a new technique called CNN_GLCMNet for feature extraction. This technique relies on Convolution Neural Network (CNN) and the Gray-Level Co-Occurrence Matrix (GLCM) techniques to mine abstract features and second-order statistical texture features. Also, Singular Value Decomposition (SVD) is applied to reduce the dimensionality of the obtained features that result from CNN, Next, the GLCM method is applied to extract second-order statistical texture features. Then, these two kinds of features (abstract features and statistical features) are combined and used as input for the classifier. Two classification mechanisms have been adopted in the classification of images into normal and abnormal skin. First, the Deep Neural Network (DNN) classifier achieves the following performance evaluation metrics (accuracy 97.43%, recall 97.25%, specificity 97.59%, precision 97.53%, f1-score 97.38%). Second, the Support Vector Machine (SVM) classifier achieves the following performance evaluation metrics (accuracy 96.93%, recall 96.99%, specificity 96.94%, precision 96.76%, f1-score 96.85%). Since both classifiers have been validated against the DFU dataset using 10-fold cross-validation. The DNN classifiers with our new feature extraction technique achieve better results in terms of accuracy, specificity, precision, recall, and f1-score than in previous work. Furthermore, a comparison of DNN and SVM classifiers finds that DNN gives a better result according to performance metrics.

Keywords

Deep Learning, Diabetic Foot Ulcer, Convolution Neural Network, Gray-Level Co-Occurrence Matrix, And Support Vector Machine

RESEARCH PAPER

An Enhanced Diabetic Foot Ulcer Classification Approach Using GLCM and Deep Convolution Neural Network

Hussein A. Ismael [a,*], Nabeel H. Al-A'araji [a], Baheja Khudair Shukur [b]

[a] College of Information Technology, University of Babylon, Hillah, Babil, Iraq
[b] College of Computer Science & Information Technology, University of Kerbala, Kerbala, Iraq

Abstract

Diabetic Foot Ulcers (DFU) are considered to be a common complication of diabetes, usually resulting in the amputation of lower extremities. Therefore, diagnosing this disease at an early stage is necessary to avoid the accompanying treatment approach, and this results in a significant cost reduction for the patient. To achieve an early diagnosis of this disease, we need to classify a patient's skin as normal or abnormal. A classification process relies heavily on the extracted features. So, we proposed a new technique called CNN_GLCMNet for feature extraction. This technique relies on Convolution Neural Network (CNN) and the Gray-Level Co-Occurrence Matrix (GLCM) techniques to mine abstract features and second-order statistical texture features. Also, Singular Value Decomposition (SVD) is applied to reduce the dimensionality of the obtained features that result from CNN, Next, the GLCM method is applied to extract second-order statistical texture features. Then, these two kinds of features (abstract features and statistical features) are combined and used as input for the classifier. Two classification mechanisms have been adopted in the classification of images into normal and abnormal skin. First, the Deep Neural Network (DNN) classifier achieves the following performance evaluation metrics (accuracy 97.43%, recall 97.25%, specificity 97.59%, precision 97.53%, f1-score 97.38%). Second, the Support Vector Machine (SVM) classifier achieves the following performance evaluation metrics (accuracy 96.93%, recall 96.99%, specificity 96.94%, precision 96.76%, f1-score 96.85%). Since both classifiers have been validated against the DFU dataset using 10-fold cross-validation. The DNN classifiers with our new feature extraction technique achieve better results in terms of accuracy, specificity, precision, recall, and f1-score than in previous work. Furthermore, a comparison of DNN and SVM classifiers finds that DNN gives a better result according to performance metrics.

Keywords: Deep learning, Diabetic foot ulcer, Convolution neural network, Gray-level co-occurrence matrix, Support vector machine

1. Introduction

A Diabetic Foot Ulcer (DFU) is considered one of the most common complications of diabetes. It can be described as a skin slough accompanied by complete loss of foot skin, often resulting from complications of neuropathic or/and vascular issues in patients with diabetes type 1 or 2. It has been found that occurs to (2–6%) of diabetic patients and influences as much as (34%) of them throughout the course of their lifetime [1,2]. In the United States, foot ulcers are considered a critical well-being issue influencing 5 to 6 million people who suffer from type 2 diabetes [2]. Furthermore, in 2010, approximately (73000) lower-limbs were amputated due to wounds that are in some way or other related to diabetes. According to the research in [3], more than eighty-five percent of foot amputations are related to diabetic foot ulcers.

Due to the spread of information and communication technology, many methods that are cost-

Received 9 June 2022; revised 6 August 2022; accepted 10 August 2022.
Available online 10 November 2022

* Corresponding author.
E-mail addresses: husseinyessari@uobabylon.edu.iq (H.A. Ismael), nhkaghed@itnet.uobabylon.edu.iq (N.H. Al-A'araji), baheeja.k@uokerbala.edu.iq (B.K. Shukur).

https://doi.org/10.33640/2405-609X.3268

effective for the remote detection and prevention of DFU have been introduced. One of these methods includes the utilization of automatic intelligent telemedicine frameworks, which beside the accessible healthcare-services, can give a high quality and low-cost DFU treatment [4,5].

In recent years, a tremendous progress has been observed in the field of computer vision, and machine learning (ML) and deep learning (DL) techniques. These techniques are capable of purposefully processing data and obtaining relevant information with an ability that exceeds the human brain in understanding and analysis, and thus can be used to provide accurate medical diagnoses [5,6]. Especially computer vision excels in analyzing complex medical images and identifying them from many aspects [7]. There is a great deal of interest in using these techniques within the Translational Medicine Framework (TMF) to improve translational scholars' ability to supply effective new diagnostics and therapies for healthcare [8,9].

Many authors have proposed approaches in computer vision by utilizing the techniques of image processing and other conventional methods in ML for the classification and localization of DFU skin or wound. Specifically, many studies applied the segmentation techniques to obtain color and texture features on a small area for images of DFU or wound. After that, the ML techniques are used for the classification of skin into healthy or DFU. Features that are extracted from images and used in ML techniques are affected by many factors including the resolution of image, lightness, shadow of skin verity size, and complex shape. Thus, the segmentation of the outline of ulcers and irregular wounds were found to be rather challenging when applying conventional ML solutions [6,10].

On the other hand, DL has made great progress in the detection, classification, and complete segmentation of DFU [11,12]. Many contributions have been made regarding the classification and detection of DFU. The research in [11] proposes a promising model called DFUNet which is based on a deep learning technique. It has been developed to classify the area of skin into normal and abnormal (DFU) skin. Another study developed by [13] proposes a new system to automate the DFU/wound image localization by using the technique of deep neural networks and applying it to iOS mobile application.

The DFU classification tasks face many challenges, including the following aspects: (i) the methods used to classify the image-DFU must be effective because DFU images are relatively more complex, (ii) the problem of lack of data, (iii) medical human-related decision require a highly accurate classification model. To obtain such an effective model, the good features need to be extracted to build such model. To overcome these challenges, a number of steps should be followed. First, DL techniques are used to deal with DFU complex images. Second, several techniques of data augmentation are applied to get around the lack of data. Third, CNN with SVM and GLCM techniques are utilized to extract sufficient features.

The major contributions of this study are outlined as follows:

- A new model has been developed based on the Convolution Neural Network (CNN) and Gray-Level Co-Occurrence Matrix to extract significant features for improving the classification process.
- The DFU classification performance is improved. The proposed model achieved the highest precision up to (97.5%), which outperforms other previous studies.
- The model with DNN classifier has been superior to the model with SVM classifier.

1.1. Outline of paper

The work presented in this paper can be described in the following way: After the introduction of this paper in Section 1, Section 2 presents related works, and Section 3 presents a description of the dataset and its collection and labelling. The methodology in Section 4 describes the data augmentation, feature extraction using CNN and FLCM, dimensionality reduction using SVD, and classifiers using DNN and SVM. Section 5 presents a description of the experimental study. At last, section 6 states the conclusions of this work.

2. Related works

There is many research works that contribute to the classification of DFU by means of computer vision techniques. These contributions can be summarized as follows: (i) building and developing algorithms based on Deep Learning techniques, (ii) building and developing algorithms based on Machine Learning techniques and image processing.

The authors in [6] proposed four models that make use of the hybrid convolution neural network to classify a patient's skin into either normal or abnormal. In their work, the models relied upon the network of multiple branches. These four deep aggregated models are built based on the combination of traditional and multiple branch convolutional layers. Different filter sizes are applied to parallel conv-layers on the same input images. The obtained features were concatenated to get better features for the classification.

The study in [14] applied the DFU QUTNet model, which is a new Deep Convolutional Neural Network. It has been introduced for categorizing skin automatically into normal (healthy) and abnormal (DFU) skin. In this study, the model is based on increasing the network width while retaining the network depth to extract the best features. These extracted features are used by SVM and K-Nearest Neighbors (KNN) classifiers.

In research [15], the authors proposed approaches that rely on ML methods to predict DFU. In their study, a new neural network called Extreme ML is suggested for prediction. In addition, each of KNN, ANN, and SVM are applied to predict DFU. Such an extreme ML method achieved highly accuracy score.

The researchers in [12] proposed a model for classifying and localizing the types of DFU (Ischaemia) and (infection) into normal or abnormal. In their work, the CNN model is used for feature extraction using shallow classifiers (KNN, DT, Ensemble, NB, SoftMax), after which the best classifier is selected. The YOLOv2-DFU model is used for the detection and localization of infections or ischemia.

In [16], the authors proposed a new network architecture that depends on unique stacked parallel convolution layers to classify a skin into DFU and normal skin. In their study, the model consists of three blocks of convolution layers which are parallel with different kernel sizes, so as to extract abstract features from local and global regions.

The study in [17] suggests an approach based on handcrafted ML method and ensemble CNN. In their work, a new feature descriptor called Superpixel Colour Descriptor is developed to extract color features from DFU image region for identifying Ischaemia and infection in DFU images.

In [18], the authors suggest a model based on DL frameworks to extract features and ML techniques for classifying DFU images whether or not they represent ulcerated feet. In their study, the inception-v3, VGG-16, and VGG-19 are used to train DFU images datasets for extracting features and ML for classification. It achieved high accuracy rates by applying the inception-v3 and SVM classifier.

3. Dataset

This section includes two steps: (i) collecting the dataset, and (ii) labeling the dataset. The DFU datasets are provided by [14]. First, a colored-images dataset of diabetic foot ulceration has been collected from various patients. It consists of 756 images of infected feet suffering from diabetic foot ulcer disease and healthy skin without disease, which were collected from the diabetic center of Nasiriyah's Hospital located in southern Iraq. It has moral endorsement and composed assent from all pertinent people and patients. The images were taken using a Galaxy Note 8 and an iPad with varying brightness and viewpoints, whereby the identity has been de-identified for all images that were collected and will be overseen (taking after other related approaches). Second, the areas or regions of interest are initially cut to a size of 224×224 pixels. This region could be a salient region surrounding the ulcer that involves vital tissues of both skin types, including normal and abnormal. Next, a specialist doctor labelled the regions that were cut into two ground-truth labels, namely normal and abnormal skin. Finally, a total of 1609 skin patches were collected, with 234 normal and 1067 abnormal (e.g., DFU). Fig (1) shows a number of normal and abnormal samples.

4. Methodology

This section includes the following steps: (i) data augmentation, (ii) feature extraction with convolution neural network, (iii) dimensionality reduction using singular value decomposition to reduce features that result from the previous step, (iv) application of the Gray-Level Co-Occurrence Matrix technique to extract texture features, (v) classification by means of deep neural network. Fig (2) shows a proposed model.

4.1. Data augmentation

Data augmentation is an essential pre-processing technique which is efficient in training highly discriminative deep learning models. To perform successfully, a convolution neural network demands a huge amount of labeled training data. Since the CNN parameters are not tuned enough, a small training set will result into significant overfitting. In addition, obtaining a sufficient amount of medical images is very expensive, so this technique will be used to solve the problem [14,19]. In this step, data augmentation was used to enhance the results by applying a variety of image processing methods including rotation, flipping, scaling, and shearing. The rotation ensures that the model is unaffected by the object's orientation. The input images are rotated in any direction between 0 and 360° randomly. When rotating an image, certain pixels will shift out of the image, necessitating a fill-in using the image reflected in the model. The image is

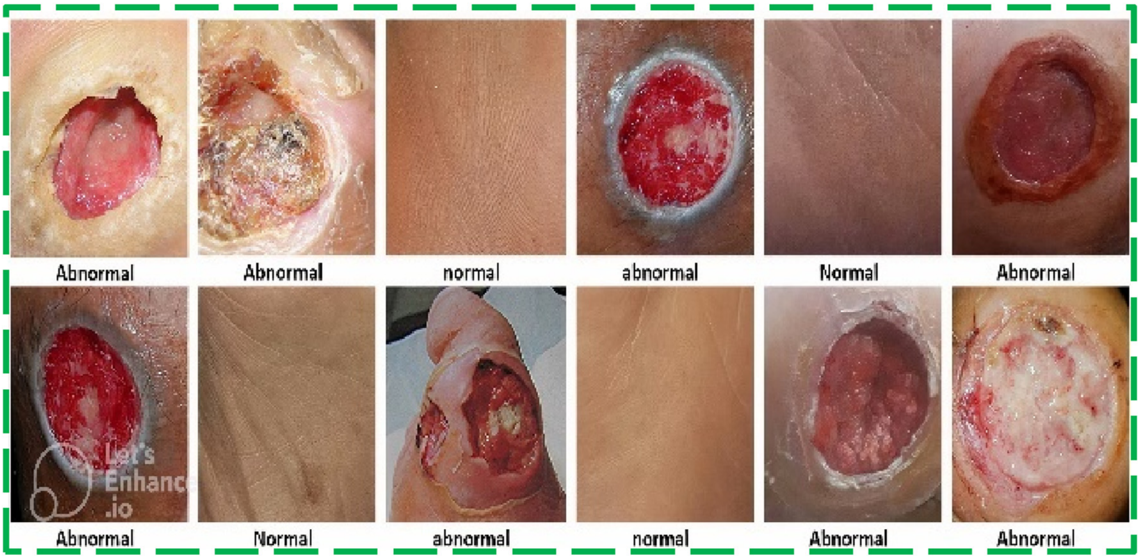

Fig. 1. Normal and abnormal samples in the dataset.

also flipped horizontally, after which the image is zoomed randomly. Shearing is typically used to enhance an image so that computers can identify how people see things from various angles. Finally, shifting the image means that an image is shifted to the left or right, bottom or up, randomly.

4.2. Feature extraction by convolution neural network

Deep Learning is considered a commonly used Machine Learning technique which makes use of a DNN. The DNN is a multi-layer neural-network that has two or more hidden layers. It differs from the traditional methods of machine learning in that the feature extraction stage is automatic instead of manual. CNN is considered one of the foremost well-known Deep Neural Network (DNN) architectures ordinarily taught by a gradient-based optimization technique. It is not only a DNN that has numerous hidden layers, but it visualizes how the cortex of the brain works in distinguishing or classifying images [20]. It comprises the serial association of the feature-extractor network and the classifier network. The feature-extractor network has accumulated pairs of convolution layers and pooling layers. The classifier network usually utilizes the common multiple-classes classification

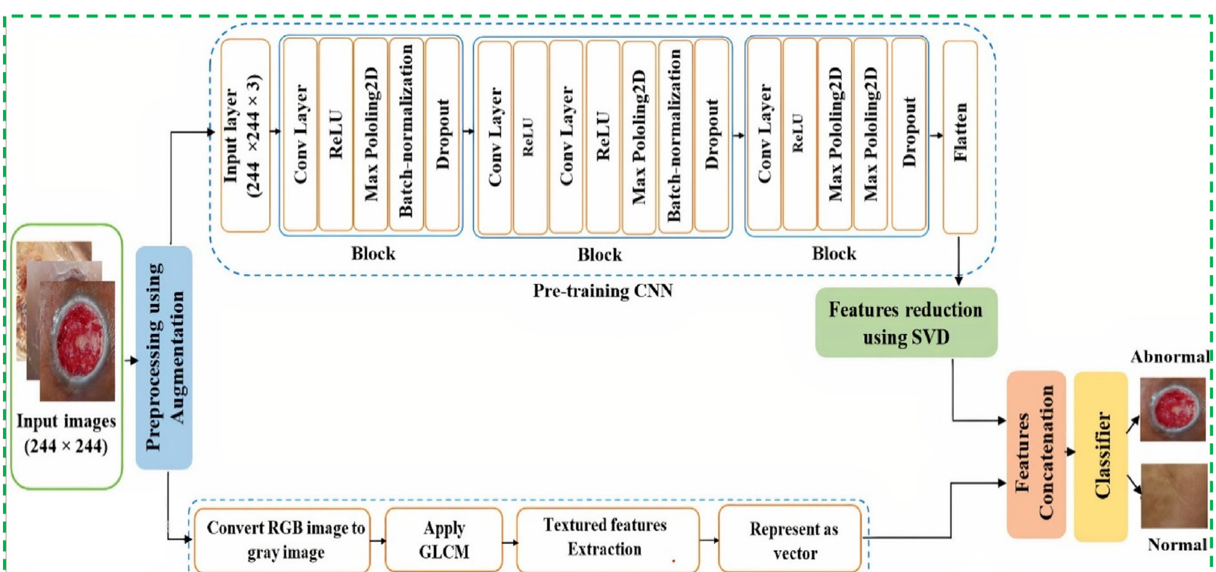

Fig. 2. Proposed model.

neural network [21,22]. In this step, a CNN model will be pre-trained to extract features from an image. Table 1 presents the architecture of the CNN pre-training model. The characteristics of the CNN pre-training model are clarified briefly as follows:

- Input layer: It is used to specify an image value corresponding to 224 × 224 × 3. These numbers refer to height, width, and the number of channels (RGB format) respectively. In this layer, data pre-processing like standardization and augmentation are based on the principle of randomly rotating, flipping, scaling, and cutting the related data. Data processing takes place before the data is entered into this layer to improve the performance of the model.
- Convolution layers: There are four convolution layers in the pretraining of the CNN model. This layer convolves the input through a set of learnable filters. Two-dimensional activation maps are created through appropriate filters, and all filters are moved across the height and width of the input volume. The filters' size has been set to 3 in all convolution layers with zero padding (e.g., it means that zeros are put around an image border to preserve its size). The model in this research comprises (4) convolutional layers with (3 × 3) filter sizes and strike (1 × 1).
- ReLu activation function: In this model, the non-linear activation function comes after the convolution layer. This function is performed by applying the max function, as follows [23].

$$Relu = \max(x, 0),\ where\ x\ input\ neuron \tag{1}$$

- Batch-normalization layer (BN): It reduces the generalization error by speeding up the training. In this model, three BN layers are used. Its working procedure involves the subtraction of the mini-batch average to be divided by the mini-batch standard deviation, so as to eventually normalize the activations of each channel. The input is then moved to the layer of BN with β (learnable offset) using γ (factor of learnable scale) to scale it [23].
- Max-Pooling layer: It mixes neighboring-pixels in a particular area of the image to create one representing value by taking the maximum pooling area. It decreases the size of the image to reduce the overfitting [24]. In this model, three layers of this type are used, and the size of the pooling area is (2 × 2).
- Dropout layer: Instead of training the complete network, only a part of the randomly selected nodes is trained. It is incredibly effective, and it is not difficult to apply. In this model, three dropping layers are used with a probability of (0.3).
- Flatten layer: It converts the dropping feature maps into a 1-D feature vector to be input into the next layer.
- Fully connected layer: They are layers in neural networks whereby the inputs from a certain layer are linked to all activation units of the next layer [23]. It has been used to combine the features that results from the flattening layer. After that, they are classified into two sets: normal and abnormal (DFU) skin.
- Sigmoid activation function: It is a nonlinear-activation function that looks the S-shape. It exists between 0 and 1. It is used to predict the probability of binary classes. This function is applied as follows [25].

$$f(x) = \frac{1}{1 + e^{-x}} \tag{2}$$

Other hyper-parameters used in this classifier are the epochs number being equal to 99 and the batch size equal to 32. The Adam optimization method is adopted with the back-propagation approach, the learning rate $lr = 0.001$, and the loss function used is the binary cross-entropy. Finally, this model has been used for pre-training the dataset so as to extract the features that can be used with GLCM features for classification.

Table 1. Architecture of CNN pre-training model.

Layer name	Output Shape	No. Parameters
Input layer	(224, 224, 3)	0
Conv layer & Relu	(224, 224, 64)	1792
Max Pooling2D	(112, 112, 64)	0
Batch-normalization	(112, 112, 64	256
Dropout	(112, 112, 64)	0
Conv layer & Relu	(112, 112, 64)	36928
Conv layer & Relu	(112, 112, 128)	73856
Max Pooling2D	(56, 56, 128)	0
Batch-normalization	(56, 56, 128)	512
Dropout	(56, 56, 128)	0
Conv layer & Relu	(56, 56, 128)	147584
Max Pooling2D	(28, 28, 128)	0
Batch-normalization	(28, 28, 128)	512
Dropout	(28, 28, 128)	0
Flatten	(100352)	0

4.3. Dimensionality reduction using singular value decomposition

The techniques to minimize the number of input variables within the training data are indicated as dimensionality reductions, such as the SVD technique. Poor performance might be caused by a huge number of input features. SVD allows for an accurate form of any matrix (M), as well as the removal of less important components within that form to obtain an approximate rank of (M) is r., whereby M is a matrix (m × n) which can be obtained for a nonzero-nonlinear combination of the rows with an all-zero vector 0. This implies that a group of columns and rows are unrelated to one another. r is the rank of M that depicts the most rows or columns with any desired number of dimensions. It is applied by means of the following formula: [26,27].

$$M_{m\times n} = U_{m\times r} \times S_{r\times r} \times (V_{n\times r})^T \tag{3}$$

Whereby U refers to a column-orthonormal matrix with m × r, S refers to a diagonal matrix, and V refers to a column-orthonormal matrix with n × r. The transposed form (V) has been used. The SVD technique is adopted for reducing the number of features produced from the pre-training CNN model, reaching a total of (512) features. After that, these features are combined with the GLCM features which are altogether used as the input to the DNN or SVD classifiers.

4.4. Gray-level Co-occurrence matrix technique

A commonly adopted texture analysis approach is the gray level co-occurrence matrix, which was initially introduced by Haralick [28]. Image features related to second-order statistics are extracted (e.g., a feature of GLCM utilizes the particular relation between two pixels in an image which are separated by a specific distance). This occurs in micro-texture regions whenever the primitive element size is large (e.g., rapidly changing value), or in macro texture regions in case the primitive element size is small (e.g., slowly changing value). A GLCM is considered a matrix (Gl), whereby the number of its rows and columns are similar to the number of gray-level ranging from (0, N-1). The number of occurrences of the pair of intensity levels i and j, at a distance apart and in the direction in the gray image, is equivalent to each entry $(i, j)^{th}$ in Gl. Adjacency can be defined as a relationship that exists in each of the four directions (horizontal, vertical, left, and right diagonal) and at any distance. Fig. 3 shows four directions of adjacency. After that the matrix (Gl) is completed, in the next step, a set of statistical measures is calculated, as follows: [28–30].

Entropy: It indicates unrest in any system, and with texture analysis, it measures the spatial unrest. It could be calculated as:

$$En_t = -\sum_{p=0}^{N-1}\sum_{k=1}^{N-1} Gl(p,k) \log Gl(p,k) \tag{4}$$

Contrast: It refers to the gray-level diversity. It can be calculated as:

$$Co_n = \sum_{p=0}^{N-1}\sum_{k=1}^{N-1} (p-k)^2 Gl(p,k) \tag{5}$$

Energy: Because energy measures local homogeneity, it is the polar opposite of Entropy. This attribute indicates how consistent the texture is. It can be calculated as:

$$En_r = \sum_{p=0}^{N-1}\sum_{k=1}^{N-1} Gl(p,k)^2 \tag{6}$$

Dissimilarity: It describes how different grey-level pairs in an original image vary. It can be calculated as:

$$Di_s = \sum_{p=0}^{N-1}\sum_{k=1}^{N-1} |p-k| Gl(p,k) \tag{7}$$

Homogeneity: It refers to the consistency of the GLCM's non-zero entries. It can be calculated as:

$$Di_s = \sum_{p=0}^{N-1}\sum_{k=1}^{N-1} \frac{1}{1-(p-k)^2} Gl(p,k) \tag{8}$$

Correlation: It denotes the image's texture similarity in two different directions, particularly, in both x and y direction directions. It can be calculated as:

$$cor_r = \frac{\sum_{p=0}^{N-1}\sum_{k=1}^{N-1} (p-m^p)(k-m^k) Gl(p,k)}{\sigma_p \sigma_k} \tag{9}$$

The data of the images are entered into the GLCM method, after converting these data images from RGB to gray, after which a GLCM matrix is calculated to extract a set of features that will be combined with the features resulting from the pre-training model. These features include Entropy, Contrast, Energy, Dissimilarity, Homogeneity, and Correlation. All these features are calculated in a variety of directions include (0°, $\frac{\pi}{4}^\circ$, $\frac{\pi}{2}^\circ$), and the variety distances include (0,1,3,5) of the Gl matrix to generate thirty features.

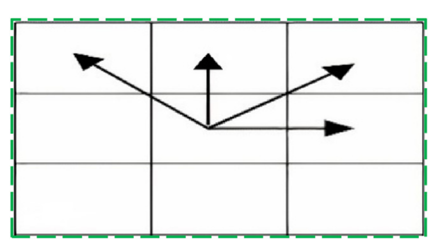

Fig. 3. Adjacency directions.

4.5. Classifiers

In this step, there are two classifiers used, including a Deep Neural Network and an SVM classifier. The features from the CNN model and GLCM approach are combined and entered as input to the DNN or SVM. The DNN consists of two input layers (GLCM features and CCN features with SVD), a concatenate layer that combines previous layers, and three dense layers after which comes the **relu** activation function immediately. This is followed by three dropouts with different probabilities (0.3, 0.5) after each dense layer aims to prevent overfitting. An output layer with sigmoid activation function is utilized to give the probability of normal or abnormal class. Another hyper-parameter used in this classifier is the learning rate $lr = 0.001$, The Adam optimization method is used with the back-propagation approach, whereby the loss function is the binary cross-entropy, the number of epochs is equal to (100), and the batch size equal to (32). Table 2 describes the layers, the number of neurons for every layer, and the number of parameters (weights). Fig (4) illustrates the architecture of DNN.

5. Experimental study

In this experiment, the Keras Tensorflow 2.4.0 has been used on Windows 10 pro for the implementation, with 8 GB NVIDIA GeForce RTX 3070Ti GPU and 16 GB DDR5 RAM. The performance of the model has been evaluated using the 10-fold cross-validation. Often, it is favored to present unbiased results because it allows the proposed model to train on multiple training-testing splits. This will give the best indicator of the model's performance for unseen samples [31,32]. The metrics have been recorded for evaluating the proposed model, including recall, specificity, precision, f1-score, and accuracy metrics. The Recall and Specificity are considered the appropriate metrics used in evaluating the model when dealing with medical images.

Table 2. Architecture of DNN model with layers no. neurons in each layer and no. of parameters.

Layer name	Output Shape	No. Parameters
Input layer1	(None, 512)	0
Input layer1	(None, 30)	0
Concat_inputs	(None, 542)	0
Dense1	(None, 128)	69504
dropout	(None, 128)	0
Dense2	(None, 128)	16512
dropout	(None, 128)	0
Dense3	(None, 64)	8256
dropout	(None, 64)	0
Output layer	(None, 1)	65

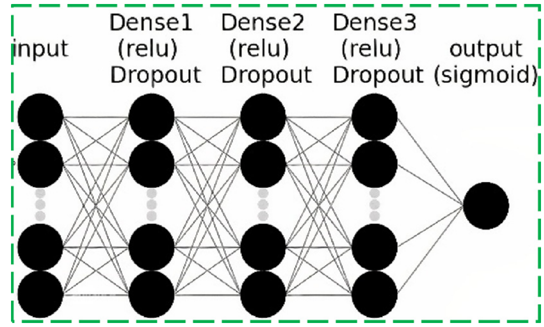

Fig. 4. DNN architecture.

The equations of evaluation metrics are as follows [33]:

$$\text{Recall} = \frac{\text{TP}}{TP + FN} \tag{10}$$

$$\text{Specificity} = \frac{\text{TN}}{FP + TN} \tag{11}$$

$$\text{Precision} = \frac{\text{TP}}{TP + FP} \tag{12}$$

$$\text{F1} - \text{Score} \ = 2 \times \frac{\text{Precision} \times Recall}{\text{Precision} + Recall} \tag{13}$$

$$\text{Accuracy} = \frac{TP + FN}{TP + \text{TN} + \text{FP} + FN} \tag{14}$$

In light of the equations above, True Positive **(TP)** occurs when an object is predicted to belong to a class, and it does indeed belong to that class. True Negative **(TN)** occurs when an object is predicted to not belong to a class and it does indeed not belong to that class. False Positive **(FP)** occurs when an object is predicted to belong to a class when in reality it does not belong to it. False Positive **(FP)** occurs when an object is predicted to belong to a class when in reality it does not belong to it. False Negative **(FN)** occurs an object is predicted to not belong to a class when in fact it does belong to it [33].

6. Results and discussion

The performance of the model using different classifiers, DNN and SVM, is presented in Table 4. It has been noted that the model with a DNN classifier obtained results that are higher for all measurements, as compared to the model with an SVM classifier. However, the model with SVM has fewer training parameters than the DNN classifier. Table 3 indicates the difference between the proposed models and other models in terms of the performance measurements. The proposed models are

Table 3. Compression between our models and others.

Model	Accuracy	Specificity	Precision	Recall	F1-Score
Hybrid DCNN with four branches [6]	–	–	97.3%	94.5%	95.8%
Hybrid DCNN with five branches [6]	–	–	96.5%	94.2%	95.3%
Hybrid DCNN with three branches [6]	–	–	94.7%	92.9%	93.7%
Hybrid DCNN with two branches [6]	–	–	93.6%	90.7%	92.1%
DFU_QUTNet [14]	–	–	94.2%	92.6%	93.4%
DFU_QUTNet + KNN [14]	–	–	93.8%	92.7%	93.2%
DFU_QUTNet + SVM [14]	–	–	95.4%	93.6%	94.5%
DFU_SPNet [16]	96.4%	95.1%	92.6%	98.4%	95.4%
SPCD + Ensemble CNN [17]	90.3%	92.1%	91.8%	–	90.2%
DFUNet [37]	90.7%	90.3%	86.7%	–	86.7%
VGG16 [34]	–	–	92.3%	89.7%	90.9%
AlexNet [35]	–	–	91.1%	87.2%	89.1%
GoogleNet [36]	–	–	95.6%	90.5%	92.9%
CNN_GLCMNet + DNN	**97.4%**	**97.5%**	**97.5%**	97.2%	**97.3%**
CNN_GLCMNet + SVM	96.9%	96.9%	96.7%	96.9%	**96.8%**

Table 4. The model with different classifiers.

The Model	Accuracy	Specificity	Precision	Recall	F1-Score
CNN_GLCMNet + DNN	97.4%	97.5%	97.5%	97.2%	97.3%
CNN_GLCMNet + SVM	96.9%	96.9%	96.7%	96.9%	96.8%

compared with the latest approaches for DFU classification, including Hybrid DCNN with (2, 3, 4.5) branches in [6], DFU_QUTNet [14], DFU_SPNet [16], Ensemble CNN [17], and DFUNet [37], and with transfer learning models such as (AlexNet, VGG16, GoogleNet). It turned out that the proposed model with the DNN classifier outperformed these models in terms of performance measures, except for the recall metric with the DFU_SPNet model. High performance scores were obtained (97.4%, 97.5%, 97.5%, and 97.3%) for accuracy, specificity, precession, and f1-score respectively, as shown in Fifure (6). The proposed model with an SVM classifier also achieved a high score for f1-score, up to 96.8% in comparison with all previous models. The model of hybrid DCNN with four branches [6] achieved lower scores in precision, recall, and f1-score, being 97.3%, 94.5%, and 95.8%, respectively, in comparison with our model with the DNN classifier. The proposed models also outperformed the hybrid DCNN with three, two, and five branches. The DFU_QUTNet model in [14] achieves lower scores for precision, recall, and f1-score, which are 94.2%, 92.6%, and 93.4%, respectively, as compared to the proposed model with DNN and SVM classifiers. Furthermore, when compared to our models, the DFU_QUTNet with SVM and DFU_QUTNet with KNN achieve low performance scores. Except

Fig. 5. Process of predication of some test images with CNN_GLCMNet + DNN model.

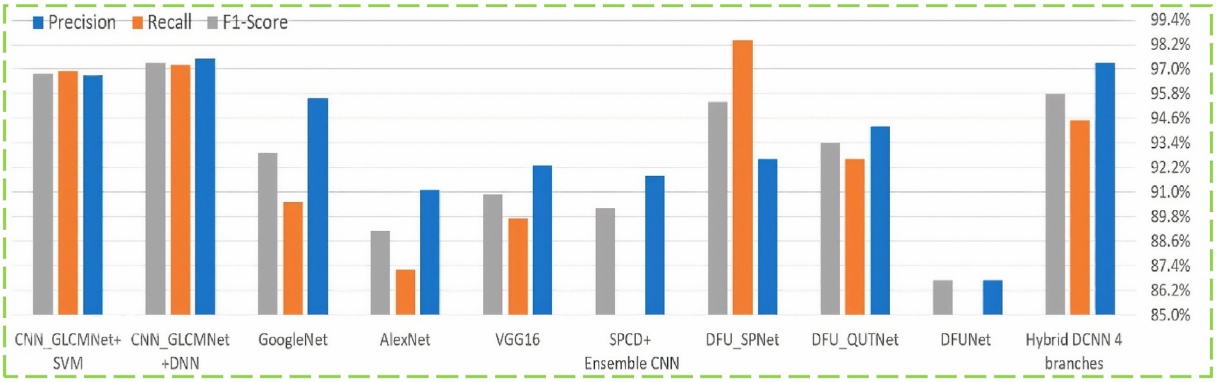

Fig. 6. Comparison the result evaluation of performance measurements.

for the recall metric (98.4%), the DFU_SPNet model in [16] gets lower scores for accuracy, specificity, precision, and f1-score (96.4%, 95.1%, 92.6%, and 95.4%, respectively). The SPCD + Ensemble CNN model [17] achieved lower scores in comparison to the proposed model with DNN in accuracy, specificity, precision, and f1-score (being 90.3%, 92.1%, 91.8%, and 90.2% respectively). The DFUNet model [37] achieved lower scores as compared to the proposed model with DNN and SVM in terms of accuracy, specificity, precision, and f1-score (being 90.7%, 90.3%, 86.7%, 86.7% respectively). AlexNet, GoogleNet, and VGG16 models all achieved lower scores in precision, recall, and f1-score. The model proposed in this work, CNN_GLCMNet + DNN, offers high performance with samples of DFU images that come from a test dataset. The correct prediction for some samples of DFU images from the test dataset is shown in Fig. (5). Therefore, the results presented by this model indicate that its results are very significant and consistent in all performance evaluation measures. In addition, use of the 10-fold cross-validation method gives the model great reliability, generalization, and unbiasing in performance (see Fig. 6).

7. Conclusions

Through this work, a new CNN_GLCMNet technique is proposed, which is determined by the new CNN architecture with SVD and GLCM to extract significant features, including abstract and texture features. Two classifiers have been proposed using a new technique of feature extraction introduced in this work. The first model, called CNN_GLCMNet + DNN, has yielded favorable results in DFU-image classification. Furthermore, the results of the empirical study showed that the performance of the CNN_GLCMNet + DNN model in classifying DFU images is enhanced in comparison with other previously published models. It has been proven that this model produces high precision and f1-score metrices, which are up to 97.5% and 97.3%, respectively. This is due to the sufficient features obtained from CNN and GLCM techniques with the DNN classifier. The second model introduced is called CNN_GLCMNet + SVM. In comparison with previous published works, the CNN_GLCMNet + SVM model achieves a higher f1-score metric, which is up to 97.3%. Finally, a comparison was drawn between our proposed models. The finding is that the CNN_GLCMNet + DNN model achieves a better overall performance than CNN_GLCMNet + SVM in terms of evaluation metrics. In light of the collected results, as well as several comparative evaluation methodologies based on prior studies, it is demonstrated that the proposed method is effective and efficient in DFU image classification. The CNN and GLCM techniques with the DNN classifier have outperformed any alternative previous methodologies.

Conflict of interest

There is no conflict of interest.

References

[1] L. Wang, P.C. Pedersen, D. Strong, B. Tulu, E. Agu, Wound image analysis system for diabetics, Med. Imaging 2013 Image Process 8669 (2013) 866−924, https://doi.org/10.1117/12.2004762.

[2] N. Al-Garaawi, R. Ebsim, A.F.H. Alharan, M.H. Yap, Diabetic foot ulcer classification using mapped binary patterns and convolutional neural networks, Comput. Biol. Med 140 (2022) 105055, https://doi.org/10.1016/J.COMPBIOMED.2021.105055.

[3] J. Apelqvist, J. Larsson, What is the most effective way to reduce incidence of amputation in the diabetic foot? Diabetes. Metab. Res. Rev 16 (2000) 75−83, https://doi.org/10.1002/1520-7560(200009/10)16:1+<::aid-dmrr139>3.0.co;2-8.

[4] D. Leightley, J.S. McPhee, M.H. Yap, Automated analysis and quantification of human mobility using a depth sensor, IEEE J. Biomed. Heal. Informatics 21 (2017) 939−948, https://doi.org/10.1109/JBHI.2016.2558540.

[5] M. Goyal, N.D. Reeves, S. Rajbhandari, M.H. Yap, Robust methods for real-time diabetic foot ulcer detection and localization on mobile devices, IEEE J. Biomed. Heal. Informatics 23 (2019) 1730−1741, https://doi.org/10.1109/JBHI.2018.28 68656.
[6] L. Alzubaidi, A.A. Abbood, M.A. Fadhel, O. Al-Shamma, J. Zhang, Comparison of hybrid convolutional neural networks models for diabetic foot ulcer classification, J. Eng. Sci. Technol 16 (2021) 2001−2017, https://doi.org/10.2139/ssrn.4010975.
[7] L. Alzubaidi, M.A. Fadhel, S.R. Oleiwi, O. Al-Shamma, J. Zhang, DFU_QUTNet: diabetic foot ulcer classification using novel deep convolutional neural network, Multimed. Tools Appl. 79 (2019) 15655−15677, https://doi.org/10.1007/S11042-019-07820-W.
[8] S. Brogi, V. Calderone, Artificial intelligence in translational medicine, Int. J. Transl. Med 1 (2021) 223−285, https://doi.org/10.3390/IJTM1030016.
[9] M. Mediouni, D.R. Schlatterer, H. Madry, M. Cucchiarini, B. Rai, A review of translational medicine. The future paradigm: how can we connect the orthopedic dots better? Current Medical Research and Opinion 34 (2017) 1217−1229, https://doi.org/10.1080/03007995.20 17.1385450.
[10] T.R. Dargaville, B.L. Farrugia, J.A. Broadbent, S. Pace, Z. Upton, N.H. Voelcker, Sensors and imaging for wound healing: a review, Biosens. Bioelectron 41 (2013) 30−42, https://doi.org/10.1016/J.BIOS.2012.09.029.
[11] M. Goyal, N.D. Reeves, A.K. Davison, S. Rajbhandari, J. Spragg, M.H. Yap, DFUNet: convolutional neural networks for diabetic foot ulcer classification, IEEE Trans. Emerg. Top. Comput. Intell 4 (2018) 728−739, https://doi.org/10.1109/tetci.2018 .2866254.
[12] J. Amin, M. Sharif, M.A. Anjum, H.U. Khan, M.S.A. Malik, S. Kadry, An integrated design for classification and localization of diabetic foot ulcer based on CNN and YOLOv2-DFU models, IEEE Access 8 (2020) 228586−228597, https://doi.org/10.1109/ACCESS.2020.3045732.
[13] D.M. Anisuzzaman, Y. Patel, J.A. Niezgoda, S. Gopalakrishnan, Z. Yu, A mobile app for wound localization using deep learning, IEEE Access 10 (2022) 61398−61409, https://doi.org/10.1109/acces s.2022.3179137.
[14] L. Alzubaidi, M.A. Fadhel, S.R. Oleiwi, O. Al-Shamma, J. Zhang, DFU_QUTNet: diabetic foot ulcer classification using novel deep convolutional neural network, Multimed. Tools Appl 79 (2020) 15655−15677, https://doi.org/10.1007/s11042-019-07820-w.
[15] S.S. Reddy, G. Mahesh, N.M. Preethi, Exploiting machine learning algorithms to diagnose foot ulcers in diabetic patients, EAI Endorsed Trans. Pervasive Heal. Technol 7 (2021) 1−14, https://doi.org/10.4108/eai.24-8-2021.170752.
[16] S.K. Das, P. Roy, A.K. Mishra, DFU_SPNet: a stacked parallel convolution layers based CNN to improve Diabetic Foot Ulcer classification, ICT Express 8 (2022) 271−275, https://doi.org/10.1016/j.icte.2021.08.022.
[17] M. Goyal, N.D. Reeves, S. Rajbhandari, N. Ahmad, C. Wang, M. H. Yap, Recognition of ischaemia and infection in diabetic foot ulcers: dataset and techniques, Comput. Biol. Med 117 (2020) 103616, https://doi.org/10.1016/j.compbiomed.2020.103616.
[18] S. Mohanty, S. Goel, R. Nijhawan, S. Gupta, Identification of diabetic foot ulcer in images using machine learning, in: 2021 19th OITS International Conference on Information Technology, OCIT. 2022, pp. 221−225, https://doi.org/10.1109/OCIT534 6 3.2021.00052.
[19] P. Chlap, H. Min, N. Vandenberg, J. Dowling, L. Holloway, A. Haworth, A review of medical image data augmentation techniques for deep learning applications, J. Med. Imaging Radiat. Oncol 65 (2021) 545−563, https://doi.org/10.1111/1754-948 5.13261.
[20] C. Janiesch, P. Zschech, K. Heinrich, Machine learning and deep learning, Electron. Mark 31 (2021) 685−695, https://doi.org/10.1007/S12525-021-00475-2/TABLES/2.
[21] A. Esteva, A. Robicquet, B. Ramsundar, V. Kuleshov, M. DePristo, K. Chou, C. Cui, G. Corrado, S. Thrun, J. Dean, A guide to deep learning in healthcare, Nat. Med 25 (2019) 24−29, https://doi.org/10.1038/s41591-018-0316-z.
[22] A. Esteva, K. Chou, S. Yeung, N. Naik, A. Madani, A. Mottaghi, Y. Liu, E. Topol, J. Dean, R. Socher, Deep learning-enabled medical computer vision, Npj Digit. Med 4 (2021) 1−9, https://doi.org/10.1038/s41 746-020-00376-2.
[23] A.M. Alhassan, W.M.N.W. Zainon, Brain tumor classification in magnetic resonance image using hard swish-based RELU activation function-convolutional neural network, Neural Comput. Appl 33 (2021) 9075−9087, https://doi.org/10.1007/S00521-020-05671-3.
[24] V. Suárez-Paniagua, I. Segura-Bedmar, Evaluation of pooling operations in convolutional architectures for drug-drug interaction extraction, BMC Bioinformatics 19 (2018) 39−47, https://doi.org/10.1186/S12859-018-2195-1/TABLES/6.
[25] H. Faris, I. Aljarah, S. Mirjalili, Training feedforward neural networks using multi-verse optimizer for binary classification problems, Appl. Intell 45 (2016) 322−332, https://doi.org/10.1007/s10489-016-07671.
[26] S. Tanwar, T. Ramani, S. Tyagi, Dimensionality reduction using PCA and SVD in big data: a comparative case study, Lect. Notes Inst. Comput. Sci. Soc. Telecommun. Eng. LNICST 220 (2018) 116−125, https://doi.org/10.1007/978-3-319 -73712-6_12.
[27] P. Lv, X. Wu, Y. Zhao, J. Chang, Noise removal for semi-airborne data using wavelet threshold and singular value decomposition, J. Appl. Geophys 201 (2022) 104622, https://doi.org/10.1016/J.JAPPGEO.2022.104622.
[28] R.M. Haralick, K. Shanmugam, I. Dinstein, Textural features for image classification, IEEE Trans. Syst. Man. Cybern, SMC- 3 (1973) 610−621, https://doi.org/10.1109/TSMC.1973.4309314.
[29] M. Partio, B. Cramariuc, M. Gabbouj, A. Visa, Rock texture retrieval using gray level co-occurrence matrix, Proc. 5th Nord. Signal Conf 75 (2002) 1−5, https://doi.org/10.1049/iet-ipr.2018.6440.
[30] S. Sachar, A. Kumar, Survey of feature extraction and classification techniques to identify plant through leaves, Expert Syst. Appl 167 (2021) 114181, https://doi.org/10.1016/J.ESWA.2020.114181.
[31] K. Pal, B.V. Patel, Data classification with k-fold cross validation and holdout accuracy estimation methods with 5 different machine learning techniques, in: 2020 Fourth International Conference on Computing Methodologies and Communication, ICCMC. 2020, pp. 83−87, https://doi.org/10.1109/ICCMC48092. 2 020.ICCMC-00016.
[32] C.I. Ossai, N. Wickramasinghe, GLCM and statistical features extraction technique with Extra-Tree Classifier in Macular Oedema risk diagnosis, Biomed. Signal Process. Control 73 (2022) 103471, https://doi.org/10.1016/J.BSPC.2021.103471.
[33] H.M. S. M.N, A review on evaluation metrics for data classification evaluations, Int. J. Data Min. Knowl. Manag. Process 5 (2015) 1−11, https://doi.org/10.5121/ijd kp.2015.5201.
[34] A. Krishnaswamy Rangarajan, R. Purushothaman, Disease classification in eggplant using pre-trained VGG16 and MSVM, Sci. Reports 10 (2020) 1−11, https://doi.org/10.1038/s4 159 8-020-59108-x.
[35] K.M. Hosny, M.A. Kassem, M.M. Fouad, Classification of skin lesions into seven classes using transfer learning with AlexNet, J. Digit. Imaging 33 (2020) 1325−1334, https://doi.org/10.1007/S10278-020-0 0371-9.
[36] C. Szegedy, W. Liu, Y. Jia, P. Sermanet, S. Reed, D. Anguelov, D. Erhan, V. Vanhoucke, A. Rabinovich, Going deeper with convolutions, in: 2015 IEEE Conference on Computer Vision and Pattern Recognition, CVPR. 2015, pp. 1−9, https://doi.org/10.1109/CVPR.2015.7298594.
[37] M. Goyal, N.D. Reeves, A.K. Davison, S. Rajbhandari, J. Spragg, M.H. Yap, DFUNet: convolutional neural networks for diabetic foot ulcer classification, IEEE Trans. Emerg. Top. Comput. Intell 4 (2018) 728−739, https://doi.org/10.1109/TETCI.2018.2866254.